PNAS RESEARCH ARTICLE | MICROBIOLOGY

Identification of basal complex protein that is essential for maturation of transmission-stage malaria parasites

Rebecca L. Clements[a,b,1], Alexander A. Morano[a,b,1], Francesca M. Navarro[a,b], James P. McGee[b,c], Esrah W. Du[b], Vincent A. Streva[b], Scott E. Lindner[c], and Jeffrey D. Dvorin[b,d,2]

Edited by L. Sibley, Washington University in St. Louis, St. Louis, MO; received March 8, 2022; accepted June 8, 2022

Malaria remains a global driver of morbidity and mortality. To generate new antimalarials, one must elucidate the fundamental cell biology of *Plasmodium falciparum*, the parasite responsible for the deadliest cases of malaria. A membranous and proteinaceous scaffold called the inner membrane complex (IMC) supports the parasite during morphological changes, including segmentation of daughter cells during asexual replication and formation of transmission-stage gametocytes. The basal complex lines the edge of the IMC during segmentation and likely facilitates IMC expansion. It is unknown, however, what drives IMC expansion during gametocytogenesis. We describe the discovery of a basal complex protein, PfBLEB, which we find to be essential for gametocytogenesis. Parasites lacking PfBLEB harbor defects in IMC expansion and are unable to form mature gametocytes. This article demonstrates a role for a basal complex protein outside of asexual division, and, importantly, highlights a potential molecular target for the ablation of malaria transmission.

Plasmodium falciparum | malaria | transmission | basal complex

Significance

Malaria, which is caused by *Plasmodium* parasites, poses a significant public health burden. *P. falciparum*, the parasite responsible for the most severe forms of malaria, undergoes substantial metamorphosis during the development of gametocyte stages, which are required for the transmission of malaria parasites. We discovered a novel protein, PfBLEB, that orchestrates parasite remodeling during the maturation of transmission stages and is required for the survival of developing gametocytes. Overall, we find that PfBLEB is important for the morphogenesis and expansion of the unique parasite cytoskeleton in *P. falciparum* gametocytes as they mature. Our findings reveal parasite cell biology and shed light on potential molecular targets for the development of drugs that could block malaria transmission.

In 2020, there were more than 200 million cases of malaria and 600,000 malaria-associated deaths (1). Several species of *Plasmodium* parasites cause human malaria, the deadliest of which is *P. falciparum* (2). Despite the abundance of available antimalarials, resistant parasites have developed for all of the drugs used in the field (3, 4), and this emerging resistance poses a threat to the treatment of malaria and, ultimately, to its eradication (5, 6). To identify targets for the rational design of antimalarial drugs, we must gain a better understanding of the fundamental biological processes that are required for the replication and development of *Plasmodium* parasites. Infection begins when a female *Anopheles* mosquito releases *P. falciparum* sporozoites from its saliva into the dermis of a human host during a blood meal (life cycle reviewed by Cowman et al. (2)). Sporozoites travel to the liver, invade hepatocytes, and undergo several rounds of replication before merozoite forms of the parasite leave hepatocytes and invade red blood cells (RBCs). The symptoms of malaria result from asexual parasite replication in human RBCs. In this 48-h cycle, *P. falciparum* progresses through ring, trophozoite, and schizont forms, then replicates to form several daughter merozoites, which are released from the RBC during egress. A fraction of ring-stage parasites develops into a transmissible form through the multistaged process of gametocytogenesis (reviewed by Meibalan and Marti (7)). After approximately 2 weeks of maturation, gametocytes are taken up by the mosquito, where they undergo sexual reproduction.

P. falciparum must faithfully undergo significant parasite cellular remodeling at multiple points in its life cycle. The ability of the parasite to remodel itself and replicate within a host cell is essential for its pathogenesis. Approximately 30 h after invading a RBC, during schizogony, the parasite undergoes several rounds of asynchronous DNA replication and karyokinesis without cytokinesis (*SI Appendix*, Fig. S1) (8). During this stage, organelles develop, divide, and are trafficked to the requisite area of the developing daughter cell. A final semisynchronized round of division occurs, and the parasite undergoes segmentation, a specialized form of cytokinesis in which individual nuclei and organelles are distributed among several daughter merozoites (8, 9). During segmentation, the plasma membrane folds in to envelop each daughter cell, but the exact mechanism behind this is not well understood. As cytokinesis is highly divergent between *Plasmodium* and humans, the proteins involved in parasite segmentation represent potential drug targets.

Another type of parasite remodeling, the development of mature gametocytes, is essential for transmission of the parasite to a mosquito, and eventually, to another human host. Stage I gametocytes are morphologically indistinguishable from asexual trophozoites (10). As the gametocyte progresses to stage II, the cell begins to elongate and lose symmetry (*SI Appendix*, Fig. S2). When the parasite reaches stage III, one

Author contributions: R.L.C., A.A.M., F.M.N., J.P.M., and J.D.D. designed research; R.L.C., A.A.M., F.M.N., E.W.D., J.P.M., and V.A.S. performed experiments; R.L.C., A.A.M., F.M.N., J.P.M., E.W.D., and V.A.S. performed research; R.L.C., A.A.M., J.P.M., S.E.L., and J.D.D. analyzed data; R.L.C., A.A.M., S.E.L., and J.D.D. wrote the paper; and all of the authors edited the paper.

The authors declare no competing interest.

This article is a PNAS Direct Submission.

[1]R.L.C. and A.A.M. contributed equally to this work.

[2]To whom correspondence may be addressed. Email: jeffrey.dvorin@childrens.harvard.edu.

This article contains supporting information online at http://www.pnas.org/lookup/suppl/doi:10.1073/pnas.2204167119/-/DCSupplemental.

Published August 16, 2022.

edge of the cell flattens, causing a D-shaped appearance and slight distortion of the RBC. Stage IV gametocytes regain cellular symmetry and are fully elongated and rigid, with pointed ends. By this stage, females and males can begin to be distinguished via standard light microscopy stains (e.g., Giemsa stain, Hemacolor stain, Field's stain) by the presence of condensed or dispersed pigmentation, respectively (11). Finally, after ∼14 d of development, mature stage V gametocytes lose their rigidity and the ends curve, forming the falciform crescent shape for which *P. falciparum* is named (10) (reviewed by Ngotho et al. (12)). Upon completion of this process, the parasite has grown several times its original size, from ∼1 μm in diameter to ∼10 μm long and ∼5 μm wide (11). The proteins that play a role in this transformation are appealing targets for antimalarial development due to the potential to abolish malaria transmission.

These parasite morphological changes are facilitated by the inner membrane complex (IMC), a membranous scaffold together with associated proteins that lie below the parasite plasma membrane, strengthen the cytoskeleton, and play a role in invasion, gametocyte formation, and cytokinesis (13). The known IMC proteins fall into two categories: glideosome-associated proteins, which link the parasite plasma membrane to the actomyosin motor, and alveolins, which form filament-like structures between the IMC and the subpellicular microtubules (13, 14). In gametocytes, the IMC serves as a critical structural support (15, 16) and disruption of the IMC blocks gametocyte development (17, 18). Members of the IMC are expressed in stage II to V gametocytes (*SI Appendix*, Fig. S2, reviewed by Dixon et al. (19)). Initially, the IMC forms a spine-like structure along only one side of the gametocyte, driving the "hat-like" appearance of stage III parasites (12), but envelops the entire gametocyte at the end of maturation, restoring cellular symmetry in stage IV to V (15, 16). Similarly, during segmentation of asexually replicating parasites, the IMC serves as a support on which daughter merozoites form (*SI Appendix*, Fig. S1) (14). In schizonts, the IMC spans the length of each fully segmented daughter merozoite, apart from the extreme polar ends. The apical end of the daughter contains a group of organelles specially equipped for the process of invading of a new RBC. At the basal end of fully segmented merozoites is the basal complex, which is believed to form a contractile ring at the edge of the emerging IMC (20).

Thus far, only two basal complex proteins, PfCINCH and PfMORN1, have been evaluated genetically in *Plasmodium* (21, 22). In addition, four other basal complex proteins have been identified and preliminarily characterized in *P. falciparum* solely via immunofluorescence microscopy: PfBCP1, PfBTP1, PfBTP2, and PfHAD2 (20, 22, 23). Thus, there is an unmet need to perform detailed functional studies on these and other basal complex proteins in *Plasmodium*. Based upon our knowledge of the basal complex in *Toxoplasma gondii*, a related apicomplexan parasite in which at least 10 basal complex proteins have been identified (23–28), it is hypothesized that several basal complex proteins in *P. falciparum* work together to facilitate the segmentation of daughter parasites (20, 27–29). In the this paper, we conduct a functional genetic evaluation of a basal complex protein and demonstrate that it plays an essential role in gametocytogenesis.

Results

Identification of PF3D7_0704300 (PfBLEB). We identified a protein, PF3D7_0704300, via a previously published immunoprecipitation of the basal complex protein PfCINCH (22), which we call PfBLEB (basolateral expansion boundary). PfBLEB has four predicted transmembrane domains clustered near the N terminus and an N-terminal signal sequence that signals for the protein to be processed through the secretory pathway (30). PfBLEB is conserved across several species of *Plasmodium* (*SI Appendix*, Table S1), but shares no homology to characterized proteins in other apicomplexans (31). Transcriptional profiling (30) and our observations via immunofluorescence microscopy (Fig. 1) demonstrate peak RNA and protein expression, respectively, approximately 35 to 40 h postinvasion, suggesting that PfBLEB may function during schizogony.

PfBLEB Is a Basal Complex Protein. Identification of PfBLEB via immunoprecipitation of the basal complex protein PfCINCH (22) led us to hypothesize that PfBLEB is a component of the basal complex. To verify this hypothesis, and to assess the localization of PfBLEB during schizogony, we fused PfBLEB to the high avidity spaghetti-monster V5 epitope tag (smV5, a dark green fluorescent protein [GFP] barrel with 10 surface-exposed copies of the V5 epitope) (32). Our characterization of PfBLEB via immunofluorescence reveals that PfBLEB forms a ring around nascent merozoites during schizogony and converges to a point at the basal end of the daughter cell as cytokinesis completes (Fig. 1). This localization pattern is typical for basal complex proteins (20, 22, 23, 29). Confirming this result, PfBLEB is in close proximity to the basal complex markers PfMORN1 (Fig. 1*A*, Pearson's R value = 0.65 ± 0.03 [mean ± SEM], $P < 0.001$) and PfCINCH (*SI Appendix*, Fig. S3*A*, Pearson's R value = 0.69 ± 0.012 [mean ± SEM], $P = 0.04$ and *SI Appendix*, Movie S1). In early segmentation, PfBLEB forms small rings near the apical end of each daughter cell (Fig. 1*A*). As segmentation progresses, these rings expand and PfBLEB continues to traverse the length of the daughter cell. Finally, the rings converge at the basal end of the newly formed merozoites as segmentation completes. Unlike PfGAP45, an IMC-associated protein, PfBLEB does not surround the entire merozoite at the end of segmentation (Fig. 1*B*). At this time, PfBLEB resides exclusively at the basal end of each daughter cell, on the opposite side of the rhoptry marker PfRON4 (*SI Appendix*, Fig. S3*B*), which labels the apical end of the merozoite. Thus, PfBLEB is a newly discovered component of the basal complex.

BLEB is conserved among several species of *Plasmodium* (*SI Appendix*, Table S1) (31). To determine whether BLEB exhibits similar expression patterns in other *Plasmodium* species, we assessed the localization of PyBLEB-GFP in *P. yoelii*. We found that PyBLEB has a dynamic localization in *P. yoelii* schizonts, mirroring the basal complex localization of PfBLEB in *P. falciparum* schizonts (*SI Appendix*, Fig. S4). This provides further evidence that BLEB is a member of the basal complex found in multiple *Plasmodium* species.

PfBLEB Is Not Required for Asexual Parasite Replication In Vitro. The basal complex is a critical component of the cellular division machinery of the parasite. Knockdown of the basal complex protein PfCINCH renders the parasite unable to replicate asexually (22). We therefore hypothesized that PfBLEB, a member of the basal complex, is important for asexual replication as well. To study the role of PfBLEB in blood-stage parasites, the PfBLEB-smV5 strain mentioned above was generated with an inducible knockdown of PfBLEB based on the Tet repressor (TetR)–binding aptamer system (33). In the absence of anhydrotetracycline (ATc), the TetR-DOZI fusion protein binds to eight copies of the TetR-binding aptamer at the 3′ end of the PfBLEB mRNA and sequesters the transcript in stress granules, which prevents translation and leads to knockdown of

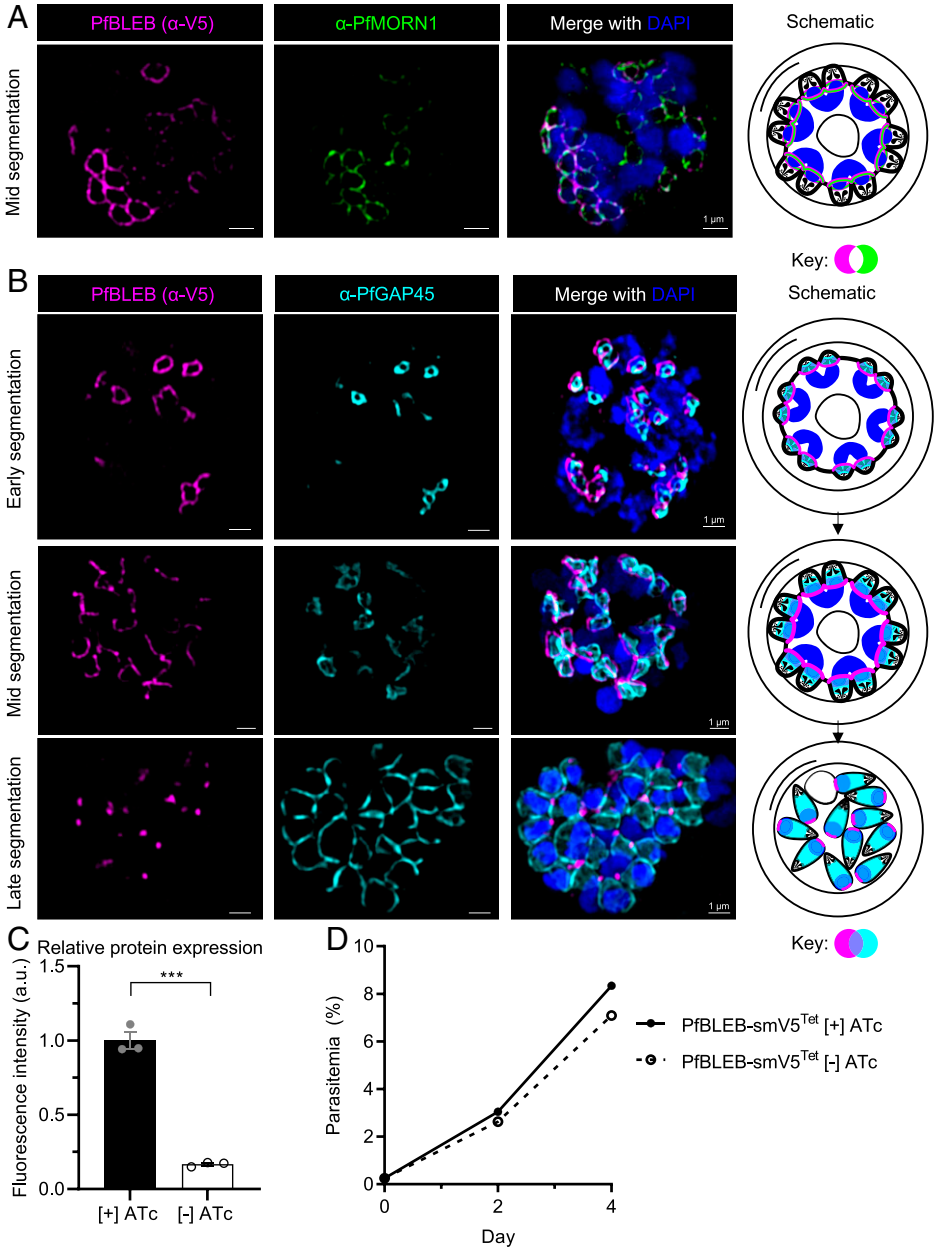

Fig. 1. PfBLEB localizes to the basal complex in asexual-stage parasites. (*A*) Immunofluorescence of PfBLEB-smV5^{Tet} shows close proximity of PfBLEB and basal complex marker, PfMORN1. (*B*) PfBLEB has distinct localization from the inner membrane complex-associated marker, PfGAP45. SR-SIM images shown are single z slices for individual channels and maximum intensity projections of merged channels. (Scale bars, 1 μm.) (*C*) Removal of ATc results in 87 ± 14% knockdown of PfBLEB-smV5 protein levels. PfBLEB-smV5^{Tet} parasites were grown in the presence or absence of ATc for 2 cycles, then immunoblot of smV5 tag in late-stage schizonts was used to quantify the level of protein knockdown. Quantification performed via volumetric measurement of fluorescence intensity with the LiCor Odyssey CLx system and fluorescence compared to histone H3 loading control. Means ± SEMs. Unpaired, two-tailed *t* test. ***$P < 0.001$. $n = 3$ technical replicates per experiment, representative of 3 independent experiments. Representative western blot shown in *SI Appendix*, Fig. S5. (*D*) Knockdown of PfBLEB via 8xTet/TetR-DOZI system does not affect asexual parasite replication. PfBLEB-smV5^{Tet} parasites were grown in the presence or absence of ATc for 2 cycles. Parasitemia was measured via flow cytometry of SYBR Green I. Means ± SDs. Error bars smaller than size of marker. $n = 3$.

PfBLEB. In the presence of ATc, TetR-DOZI preferentially binds to ATc instead of the Tet aptamers, and therefore PfBLEB is efficiently translated (33). With the removal of ATc, we see 87 ± 14% (mean ± SD) knockdown of PfBLEB protein via immunoblot of the smV5 epitope tag (Fig. 1*C* and *SI Appendix*, Fig. S5). We observe a mild, statistically insignificant, but reproducible growth defect (<5% difference in parasitemia after 2 cycles, $P = 0.26$) following the removal of ATc in PfBLEB-smV5^{Tet} parasites (Fig. 1*D*).

Given the absence of a significant growth defect upon PfBLEB knockdown, we reasoned that PfBLEB is dispensable for asexual replication in vitro, in contrast to our original hypothesis. Using selection-linked integration with targeted gene disruption (SLI-TGD) (34), we successfully disrupted the PfBLEB locus in 3D7 parasites. This two-step method relies on homologous recombination and the use of two resistance markers to first select for episomal expression of the SLI-TGD plasmid and then for integration of the plasmid and therefore gene disruption. We modified the previously described SLI-TGD plasmids to include a different selectable marker and an in-frame smV5 epitope tag attached to the first 165 amino acids, disrupting 91% of the PfBLEB coding region. Following selection, we verified integration of this construct and the resulting disruption of PfBLEB by PCR and whole-genome sequencing and confirmed expression of smV5 in late-stage parasites (*SI Appendix*, Fig. S6). It is important to note that the four transmembrane domains of PfBLEB are not disrupted in this strain. However, unlike PfBLEB, the smV5 tag does not localize to the basal complex, suggesting that the first 165 amino acids of PfBLEB are not sufficient for basal complex localization. The correct integration of this strain demonstrates that PfBLEB is not essential for asexual parasite replication in vitro and is consistent with piggyBac transposon insertion mutagenesis screening data (35).

PfBLEB Is Essential for the Formation of Mature Gametocytes. The IMC plays an important structural role in the remodeling that takes place during both segmentation and gametocyte formation. Given the essential nature of the basal complex in

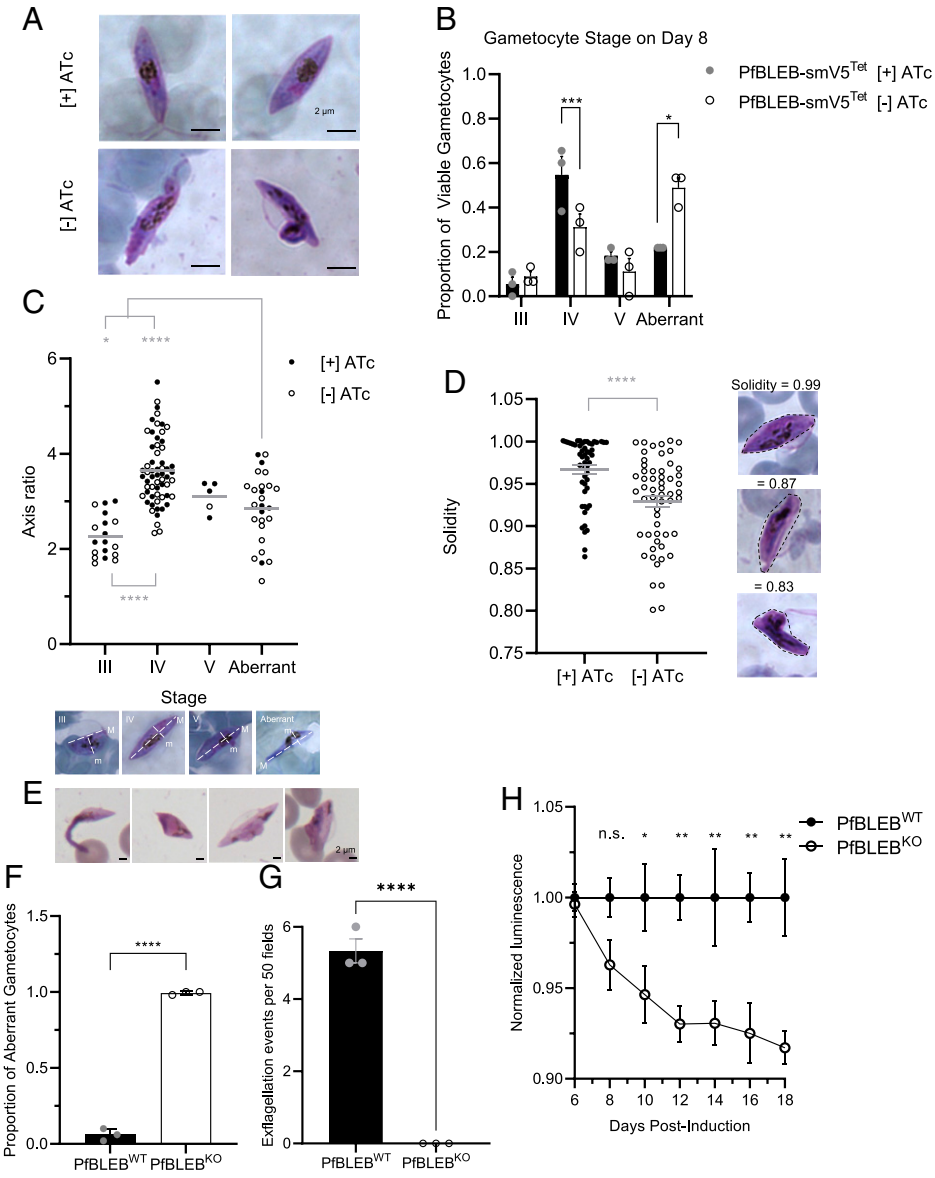

Fig. 2. PfBLEB is essential for the formation of mature gametocytes. (*A*) PfBLEB knockdown gametocytes show aberrant morphology. Gametocyte formation was induced in PfBLEB-smV5^{Tet} parasites in the presence or absence of ATc. Hemacolor stained images on Day 8 after gametocyte induction. (*B*) PfBLEB knockdown inhibits gametocyte maturation. Gametocyte stage was determined on day 8 after gametocyte induction via Hemacolor stain. Means ± SEMs. Two-way ANOVA. *P < 0.05, ***P < 0.001. n = 3 technical replicates per experiment, representative of 3 independent experiments. (*C*) PfBLEB-deficient gametocytes fail to elongate. Hemacolor-stained images were acquired 8 d postinduction in parasites grown in the presence or absence of ATc. Sixty images were taken for each condition. Axis ratio and solidity of Hemacolor-stained images was measured in ImageJ. Each individual cell is marked as a circle, grand mean (combining cells in both presence and absence of ATc) shown on the graph and used to perform a 1-way ANOVA. *P < 0.05, ****P < 0.0001. n = 3. Examples of images from each category shown below the graph, along with definition of major (M) and minor (m) axes. (*D*) PfBLEB deficient gametocytes have irregular borders. Hemacolor-stained images were acquired 8 d postinduction in parasites grown in the presence or absence of ATc. Sixty images were taken for each condition. Solidity of Hemacolor-stained images was measured in ImageJ. Each individual cell is marked as a circle. Means ± SEMs. Unpaired t test. ****P < 0.0001. n = 3. Examples of images with high and low solidities shown below the graph, along with sample convex shapes surrounding the area of each cell. (*E*). PfBLEB knockout parasites have aberrant morphology. Representative Hemacolor-stained images on day 8 after gametocyte induction. (*F*) Quantification of Hemacolor-stained gametocytes 10 d after gametocyte induction in PfBLEB^{KO} and wild-type 3D7 parasites. Means ± SEMs. Unpaired, 2-tailed t test. ****P < 0.0001. n = 3, 50 gametocytes counted per condition per replicate. (*G*) PfBLEB^{KO} parasites fail to exflagellate. PfBLEB^{KO} and wild-type 3D7 gametocytes were activated 14 d after gametocyte induction. Exflagellation centers were identified via α-tubulin staining. Means ± SEMs. Unpaired, 2-tailed t test. ****P < 0.0001. n = 3, fifty 60× fields counted per condition per replicate. (*H*) PfBLEB knockout parasites die during maturation. Quantification of PfBLEB^{KO} parasite viability compared to wild-type 3D7 parasites. Viability assessed using luminescent ATP assay every 2 days beginning 6 d postinduction. Luminescence normalized to wild-type parasites after subtracting luminescence of uninfected RBCs and adjusted for gametocytemia in each well. Means ± SEMs. Multiple t tests were performed for each day indicated. *P < 0.05, **P < 0.01, n.s., not significant. n = 3. Representative images of gametocytes in the aberrant category. (Scale bars, 2 μm.)

IMC expansion during schizogony, we hypothesized that the basal complex drives expansion of the IMC during gametocytogenesis as well. To test this hypothesis and investigate the role of the basal complex in gametocyte development, we followed gametocytogenesis with and without ATc in PfBLEB-smV5^{Tet} parasites. As a control, we see no impact on gametocyte development in wild-type 3D7 with or without ATc added to the culture media (*SI Appendix*, Fig. S7*A*). However, gametocytes that form in the absence of PfBLEB demonstrate aberrant morphology, indicating that PfBLEB expression is important for gametocytogenesis (Fig. 2*A*). While PfBLEB-smV5^{Tet} gametocytes with and without ATc look similar in stages I and II, they begin to deviate beginning in stage III, and aberrant gametocytes that possess large membrane blebs or jagged edges begin to accumulate in PfBLEB-deficient conditions.

To quantify these aberrancies in an unbiased manner, we used three measurements: symmetry, axis ratio, and solidity. Axis ratio (the length of major axis divided by the length of the minor axis) is a measure of elongation. As the gametocyte matures (stages I to IV), the axis ratio increases as the parasite elongates. In stage V, when the microtubules are broken down, the ends of the parasite curve and the axis ratio decrease (15). Solidity is a measure of the density of a shape. It is calculated by dividing the area of a shape by the area of the smallest possible convex shape that will enclose the shape. Solidity close to 1 indicates high shape density, which means that the borders surrounding the cell are smooth and convex and that the shape is solid. Smaller solidity indicates low shape density, which reflects irregular or concave borders. The following traits were used to categorize cells according to stage: normal stage II parasites have 2 perpendicular axes of symmetry, an axis ratio close to 1 (slightly elongated), and solidity close to 1 (regular, convex borders). Normal stage III parasites have 1 axis of symmetry, an axis ratio close to 2 (as they begin to elongate further), and solidity close to 1. Normal stage IV parasites have 2 perpendicular axes of symmetry, an axis ratio of ~2 to 5 (fully elongated), and solidity close to 1. Normal stage

V parasites have 1 or 2 axes of symmetry (depending on how curved the parasite is), an axis ratio close to 3 (as the ends curve and the cell loses some elongation), and solidity close to 1. In stages IV and V, females have condensed pigmentation and males have dispersed pigmentation. Aberrant parasites, by our definition, are categorized based on gross abnormalities—membrane blebs or lack of symmetry.

Using these guidelines, more than half of PfBLEB-deficient gametocytes were categorized as aberrant 8 d postinduction, in contrast to only ∼20% of gametocytes grown in the presence of ATc (Fig. 2*B*). This accumulation of aberrant gametocytes results in a significant decrease in mature stage IV and V gametocytes (Fig. 2*B* and *SI Appendix*, Fig. S7*B*). In the aberrant parasites we analyzed, the mean axis ratio lies between the range of normal stage III and stage IV gametocytes (Fig. 2*C*). This reflects a failure of these cells to elongate during the transition from stage III to stage IV. In addition, solidity is significantly lower in the parasites grown without ATc, indicating that PfBLEB knockdown parasites have a higher incidence of irregular, concave borders (Fig. 2*D*). In the gametocytes that are able to mature to stage IV or V, the ratio of females to males in the parasites grown in the presence of ATc is roughly equal to the female-to-male ratio in parasites grown in the absence of ATc (∼8:1 in this strain, compared to ∼4:1 ratio, which we observe in wild-type 3D7).

As noted above, the level of knockdown in the PfBLEB-smV5^{Tet} strain is incomplete (65 ± 18% [mean ± SD], *SI Appendix*, Fig. S5*C*). To overcome this, we monitored gametocyte maturation in our PfBLEB knockout strain. As predicted, the aberrant phenotype is even more apparent in the PfBLEB knockout parasites. Much like PfBLEB knockdown, PfBLEB knockout parasites develop on par with wild-type 3D7 parasites until early stage III. However, the parasites fail to transition from stage III to stage IV and begin to show phenotypic aberrancies 6 to 8 d postinduction (Fig. 2*E*). By 10 d postinduction, 149/150 gametocytes counted had an aberrant phenotype (and 1/150 was a phenotypically normal, albeit potentially delayed, stage IIb gametocyte) (Fig. 2*F*). After multiple biological and technical replicates, we were not able to find a single stage IV or stage V gametocyte in our PfBLEB knockout strain, even up to 18 d postinduction. In addition, we find that PfBLEB knockout gametocytes fail to exflagellate, demonstrating a functional defect in addition to phenotypic aberrancies (Fig. 2*G*). Thus, we have demonstrated that PfBLEB is required for the formation of mature, functional stage V gametocytes. These abnormal PfBLEB knockout gametocytes also begin to die within 8 d after gametocyte induction, demonstrating that PfBLEB is important for gametocyte viability (Fig. 2*H*). Concurrent with this finding, in our inducible PfBLEB-smV5^{Tet} knockdown strain, parasites are unable to recover if ATc is added back to the culture media during stage III (*SI Appendix*, Fig. S7*C*). Overall, these findings demonstrate that PfBLEB is required for the formation of mature, viable gametocytes.

PfBLEB Lines the Leading Edge of the Expanding IMC Throughout Gametocytogenesis. The basal complex localizes to the edge of the expanding IMC during segmentation of asexual-stage schizonts, but the expression of a basal complex protein outside of schizogony has not previously been demonstrated. To test our hypothesis that PfBLEB also associates with the IMC in gametocytes, we investigated the localization of PfBLEB during gametocytogenesis. Our assessment of PfBLEB by immunofluorescence microscopy during gametocyte maturation reveals a dynamic membrane-associated localization (Fig. 3). Using immunofluorescence, we find that PfBLEB-smV5 initially lines one edge of stage II gametocytes. The IMC then forms on the opposite side of the cell, visualized via PfGAP45 staining. PfBLEB staining expands along the membrane and begins to envelop the cell until it reaches the edge where PfGAP45 resides. Microtubules then assemble beneath the IMC, causing that edge of the gametocyte to straighten and form the characteristic "D" shape present in stage III. As the IMC and microtubule network expands and the gametocyte continues to mature, PfBLEB converges such that PfGAP45 and PfBLEB staining never overlap. Mirroring its role during segmentation of asexual-stage parasites, PfBLEB converges to a single point on the periphery of stage IV gametocytes and the IMC surrounds the remainder of the cell. The microtubules are then disassembled as the gametocyte transitions from stage IV to stage V, and PfBLEB staining disappears.

Knockdown of PfBLEB Disrupts Expansion of the IMC and Microtubules in Gametocytes. Elongation of the *P. falciparum* gametocyte into the characteristic crescent shape relies on recruitment of the IMC and formation of a network of cortical microtubules (15, 18). Thus, the IMC is critical for parasite cellular remodeling during gametocytogenesis. Given the interaction between the IMC and basal complex during segmentation, we hypothesized that the aberrant phenotypes that we observe in PfBLEB knockdown and knockout parasites may reflect improper IMC expansion in gametocytes. Consistent with our hypothesis, by immunofluorescence, we observe aberrant localization of IMC- and microtubule-associated markers in PfBLEB-deficient gametocytes (Fig. 4*A* and *SI Appendix*, Fig. S8). Phenotypically normal stage IV gametocytes have evenly spaced, longitudinally oriented microtubules on the periphery of the cell under the cytoplasmic face of the IMC. In PfBLEB-deficient parasites, while both the IMC and microtubules are present, the cytoskeletal network demonstrates aberrant localization, which by our definition includes microtubules that do not run longitudinally or that have an angle of curvature greater than 90 degrees. Using these guidelines, we observe aberrant α-tubulin staining in more than 20% of PfBLEB-smV5^{Tet} gametocytes grown in the absence of ATc (compared to less than 10% in gametocytes grown in the presence of ATc; Fig. 4*A*).

These findings are further supported via transmission electron microscopy (TEM), with which we observe aberrant appearance of the IMC and microtubules on an ultrastructural level (Fig. 4*B* and *SI Appendix*, Figs. S9 and S10). Phenotypically normal stages III and IV gametocytes have one double bilayer of IMC within 20 nm of the plasma membrane and a single, evenly spaced (10 nm periodicity) layer of microtubules within 20 nm of the IMC. By our definition, aberrant cells meet one of the following qualifications: IMC greater than 20 nm away from the plasma membrane, more than 1 layer of microtubules, uneven spacing of microtubules or lack of 10 nm periodicity, or microtubules greater than 20 nm away from the IMC. We see a range of phenotype severity in the knockdown condition, which is reflective of the abnormalities we observe via immunofluorescence microscopy. Overall, these data demonstrate that PfBLEB is essential for the expansion of the IMC and microtubule network in maturing gametocytes.

PfBLEB Does Not Colocalize with Known Members of the Asexual Basal Complex in Gametocytes. Six other proteins in addition to PfBLEB have been shown to localize to the basal complex during segmentation of asexual stage parasites, but

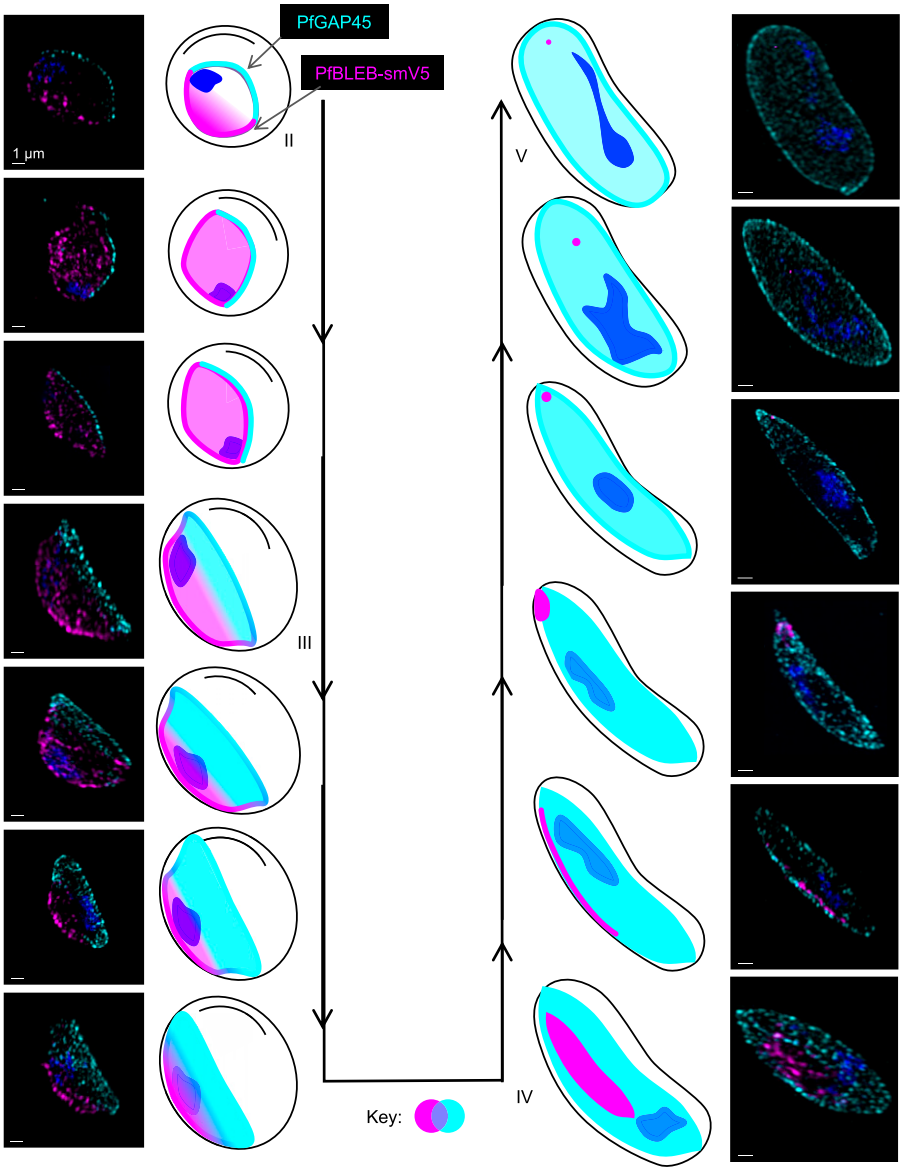

Fig. 3. PfBLEB marks the leading edge of the inner membrane complex as it expands during gametocyte formation. Immunofluorescence of PfBLEB-smV5^{Tet} (magenta) lines the edge of the inner membrane complex (IMC) and contracts as the IMC envelops the developing gametocyte. PfGAP45 (cyan) is an IMC-associated protein. Maximum intensity projections of SR-SIM images from day 4 (images 1 to 5, 7 to 10), 6 (images 6, 11), 8 (image 12), or 10 (image 13) after gametocyte induction. (Scale bars, 1 µm.)

their expression has not yet been evaluated in gametocytes (20, 22, 23, 25, 29). To determine whether other known basal complex proteins also play a role in gametocyte maturation, we assessed the localization of four of these six proteins (PfCINCH, PfMORN1, PfBCP1, and PfBTP2) in transmission-stage parasites via immunofluorescence (using PfCINCH-smMyc or PfBTP2-3xHA parasite strains or primary antibodies against PfMORN1 or PfBCP1 (22)). RNA transcripts for PfCINCH, PfMORN1, and PfBTP2 have been detected previously in mature gametocytes (36). While we find that each of these proteins localize to the leading edge of the emerging IMC in schizonts, only PfCINCH is detected during gametocytogenesis by immunofluorescence (Fig. 5 and *SI Appendix*, Fig. S11). However, PfCINCH and PfBLEB are not expressed in the same subcellular location in gametocytes. Unlike the dynamic membrane localization of PfBLEB, PfCINCH forms punctate structures throughout the cytoplasm in stage II to stage V gametocytes, and this staining is not altered as the IMC envelops the cell (Fig. 5). In contrast to PfBLEB, which marks the areas of the plasma membrane that are devoid of PfGAP45, PfCINCH staining lies inside PfGAP45 staining as the gametocyte matures. In addition, PfCINCH is expressed throughout the cytoplasm in fully mature gametocytes, while PfBLEB is not expressed in fully mature gametocytes. This finding suggests that while some core components of the basal complex are expressed during both the asexual and transmission stages, these proteins do not interact in the same way in both life cycle stages, and likely serve separate functions in gametocytes.

Proximity-Dependent Biotinylation Reveals Proteins that Reside Near PfBLEB. Given the unique localization and critical function of PfBLEB during gametocytogenesis, we aimed to identify other proteins that comprise this novel subcellular compartment. Using the TurboID proximity-dependent biotin ligase (37), we identified proteins in close proximity to PfBLEB in both schizonts and gametocytes. We confirmed that fusion of the TurboID ligase to the carboxy-terminus of endogenous PfBLEB does not alter its localization in either schizonts or gametocytes (*SI Appendix*, Fig. S12). We performed proximity labeling in 3D7-PfBLEB-TurboID schizonts during late segmentation (~46 h postinvasion) and identified 95 proteins shared among 2 replicates (*SI Appendix*, Fig. S13) (38). We found several known IMC and basal complex proteins highly

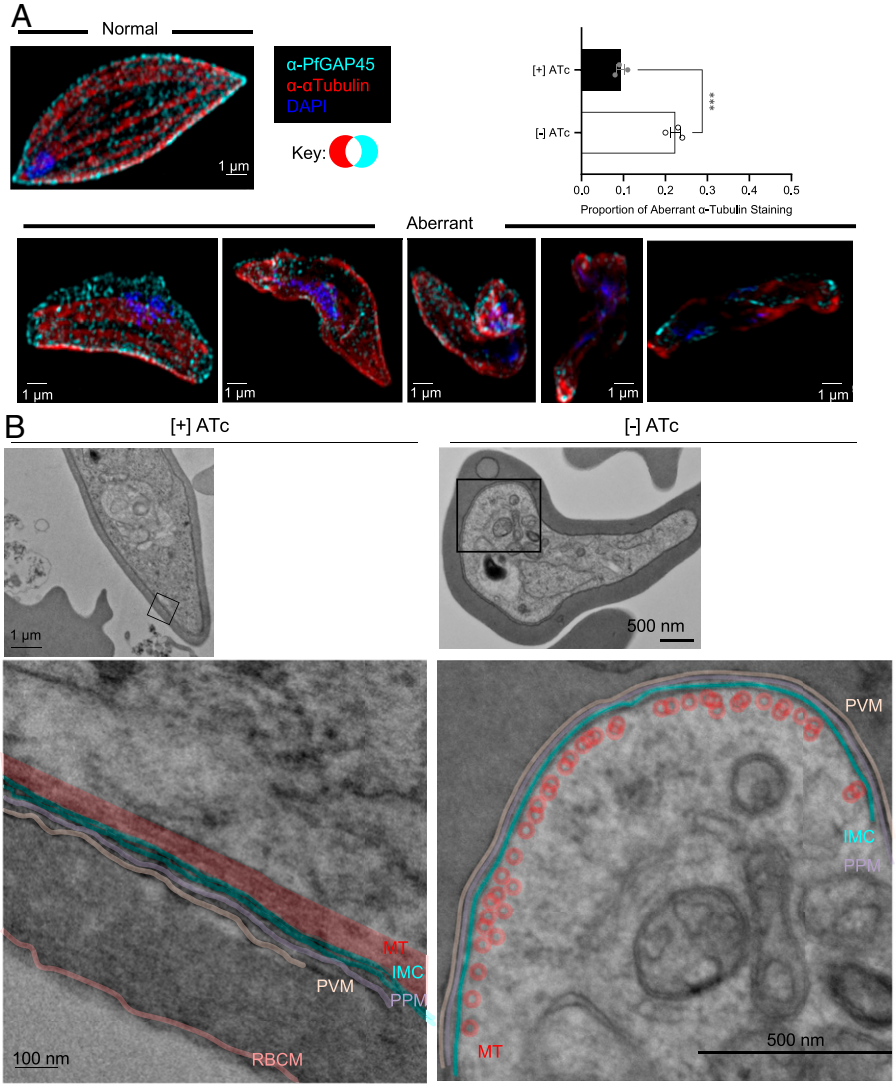

Fig. 4. Knockdown of PfBLEB disrupts the expansion of the inner membrane complex and microtubule network in gametocytes. (*A*) Gametocyte formation was induced in PfBLEB-smV5^{Tet} parasites in the presence or absence of ATc. Immunofluorescence of α-tubulin (red) and PfGAP45 (cyan) on day 10 after gametocyte induction demonstrates an incohesive microtubule network in PfBLEB knockdown parasites. Images were categorized and quantified, demonstrating a significant difference in the proportion of aberrant α-tubulin staining in gametocytes grown in the presence or absence of ATc. Means ± SEMs. Unpaired, 2-tailed *t* test. ****$P < 0.0001$. $n = 3$ technical replicates per experiment, representative of 3 independent experiments. Fifty gametocytes counted per condition per replicate. Example images from normal and aberrant categories shown as maximum intensity projections of SR-SIM images. (Scale bars, 1 μm.) (*B*) TEM of gametocytes grown in the presence or absence of ATc on day 8 after gametocyte induction. One representative cell from the [+] ATc condition (left) and the [–] ATc condition (right) shown. Magnified sections shown beside and/or below the image. Color added on top of image to emphasize features. Original, noncolored versions in *SI Appendix*, Fig. S9. MT = subpellicular microtubules, red; IMC = inner membrane complex, cyan; PPM = parasite plasma membrane, purple; PVM = parasitophorous vacuolar membrane, tan; RBCM = RBC membrane, pink. Representative images of gametocytes in the aberrant category.

represented in our data, bolstering our confidence in the biological significance of our results (*SI Appendix*, Table S2).

We performed proximity labeling in stage II-III NF54-PfBLEB-TurboID gametocytes. Initially, these parasites were cultured in the absence of biotin from the onset of transfection. Biotin was added only for the duration of the proximity labeling experiment. To remove potential artifacts caused by a long period of growth in the absence of biotin and to confirm that lack of biotin does not hinder gametocyte development, we cultured NF54-PfBLEB-TurboID parasites in the presence of biotin for >10 replication cycles, then repeated our proximity labeling experiment in biotin-free media. Our second replicate had higher levels of background, likely caused by residual biotin from the culture media. However, 65 proteins remained consistent between both replicates (Fig. 6*A* and *B*). We compared consensus proteins from schizont and gametocyte samples and identified 25 proteins shared between all 4 experiments (2 schizont replicates and 2 gametocyte replicates, *SI Appendix*, Fig. S13).

PF3D7_1435600 Is a Protein that Does Not Localize to the Basal Complex. Proximity-dependent biotinylation revealed several uncharacterized potential near-neighbors of PfBLEB, including PF3D7_1435600. PF3D7_1435600 is conserved across several species of *Plasmodium* and is predicted to be essential for asexual replication by piggyBac transposon insertion mutagenesis screening (35). Transcriptional profiling suggests a similar expression profile to PfBLEB in schizogony (30, 31). To confirm that PF3D7_1435600 and PfBLEB reside in close proximity, we assessed the localization of PF3D7_1435600-smV5 (*SI Appendix*, Fig. S14) in schizonts and gametocytes. Interestingly, we find that PF3D7_1435600 does not localize to the basal complex during schizogony, but instead forms distinct punctae throughout segmentation (Fig. 6*C* and *SI Appendix*, Fig. S15). Throughout gametocytogenesis, PF3D7_1435600-smV5 demonstrates a staining pattern distinct from PfBLEB (Fig. 6*D* and *SI Appendix*, Figs. S16 and S17). Strikingly, while PF3D7_1435600-smV5 does have staining in the region of the gametocyte devoid of IMC (where PfBLEB localizes), this localization is overshadowed by intense staining in a different region of the gametocyte. Importantly, in all asexual and gametocyte parasites evaluated by immunofluorescence, we observe limited but consistently present regions of overlap between PF3D7_1435600 and PfBLEB, explaining the proximity labeling of PF3D7_1435600 by PfBLEB-TurboID. Thus, in both schizonts and gametocytes, PF3D7_1435600 resides in a pattern that is inconsistent with basal complex localization.

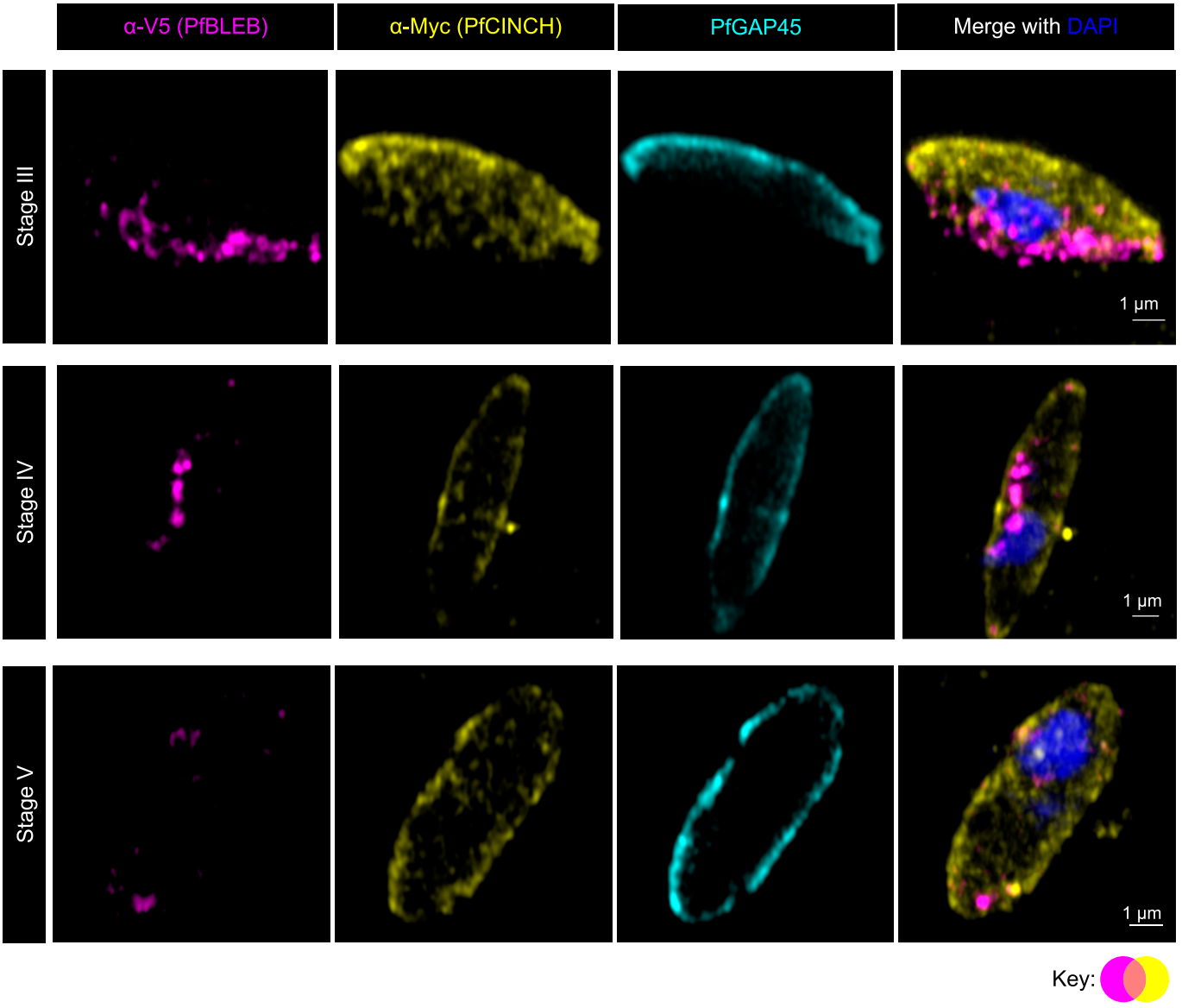

Fig. 5. PfCINCH is expressed during gametocytogenesis but does not colocalize with PfBLEB. Immunofluorescence demonstrates PfCINCH-smMyc (yellow) and PfBLEB (magenta) expression in developing gametocytes. PfGAP45 (cyan) is an IMC-associated protein. Unlike PfBLEB-smV5, which has a dynamic membrane-associated localization that contracts as the IMC expands, PfCINCH-smMyc demonstrates punctate cytoplasmic expression throughout gametocytogenesis that persists independently of IMC expansion, even in late-stage gametocytes after PfGAP45 surrounds the parasite. Airyscan images shown are single z slices for individual channels and maximum intensity projections of merged channels 8 d after gametocyte induction. (Scale bars, 1 μm.)

Discussion

To our surprise, through characterization of a basal complex protein, we demonstrate that while cytoskeletal expansion drives parasite cellular remodeling during both asexual division and sexual conversion, the molecular mechanisms in each stage are distinct. During segmentation of asexual parasites, the IMC forms at the apical pole before enveloping the nascent daughter cell, a process that is believed to be guided by contractile forces of the basal complex (16, 20, 22). Similarly, in gametocytogenesis, the IMC first forms along one edge of the developing cell, then envelops the mature gametocyte (18). We have provided evidence that a member of the basal complex, PfBLEB, is a critical player in IMC elongation during gametocytogenesis. We have demonstrated that PfBLEB contributes to expansion (but not assembly) of the IMC in gametocytes as they mature, and thus helps to orchestrate dramatic morphological remodeling during gametocytogenesis. We have shown that a basal complex protein serves a critical role in the formation of mature gametocytes. When this protein is absent, the IMC and microtubule network fails to envelop the cell, and developing gametocytes are unable to complete the necessary structural remodeling. Notably, PfBLEB knockout gametocytes show normal morphology and have equal viability as wild-type gametocytes until the IMC begins to expand (~8 d postinduction; Fig. 2*H*), demonstrating that the inability to complete maturation is linked to defects in IMC expansion.

It is remarkable that *P. falciparum* can use the same core cellular machinery (members of the IMC and basal complex) to orchestrate the distinct processes of cytokinesis and gametocyte maturation. While the localization of PfBLEB in asexual stages and gametocytes share similarities in association with the IMC, the two stages also have several distinct characteristics. During segmentation, the basal complex originates on the apical end, and progresses toward the basal end (20, 29). While the basal complex expands then contracts throughout this process, it

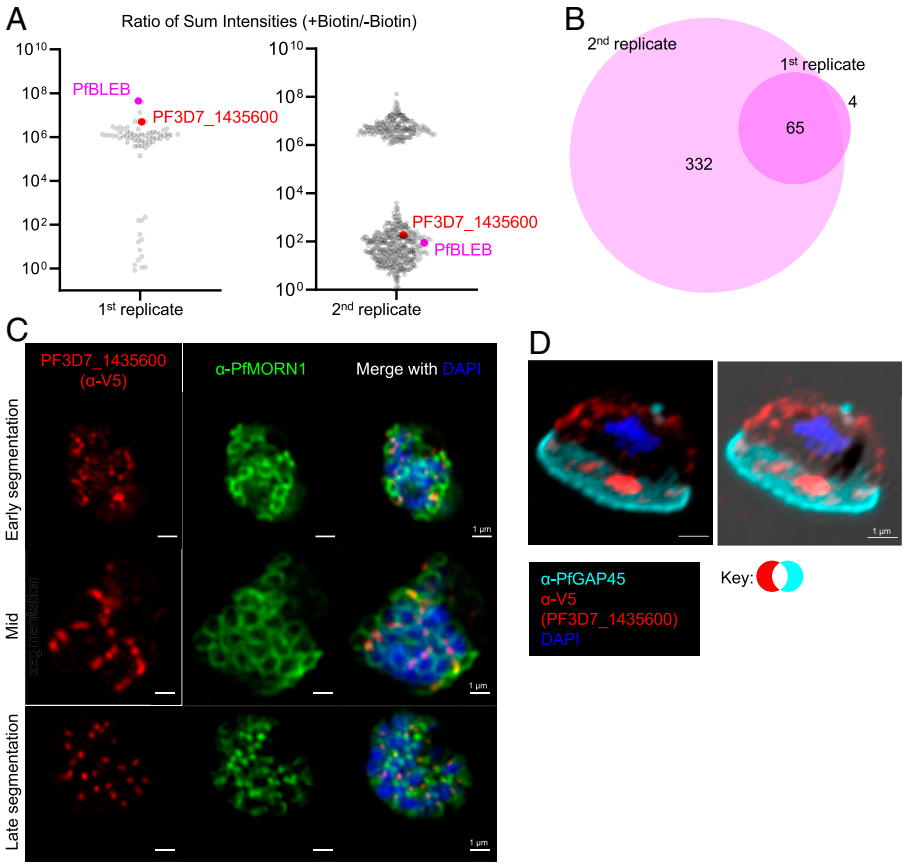

Fig. 6. Proximity-dependent biotin identification reveals proteins that reside near PfBLEB during gametocytogenesis. (*A*) Dot plots showing the ratio of the sum intensity in the presence/absence of biotin of proteins detected via mass spectrometry of PfBLEB-TurboID gametocytes. Thresholds were set to require more unique peptides than streptavidin. Sum intensity set to 1 for proteins absent in no biotin control. (*B*) An area-proportional Venn diagram comparing the proteins identified in both gametocyte TurboID replicates. (*C* and *D*) Immunofluorescence demonstrates that PF3D7_1435600-smV5 (red) localizes to distinct, punctate foci throughout schizogony (*C*) and gametocytogenesis (*D*), adjacent to basal complex protein PfMORN1 (green) or inner membrane complex-associated protein PfGAP45 (cyan). For (*C*), Airyscan images shown are single z slices for individual channels or maximum intensity projections of merged channels. For (*D*), the images shown are maximum intensity projection merged without and with brightfield image. (Scale bars, 1 μm.)

travels in the same direction throughout the entire process; it never reverses along the polar axis. In developing gametocytes, however, PfBLEB starts on one pole, expands, then reverses and contracts toward the original pole. In addition, during schizogony, the parasite must coordinate replication and partitioning of its cellular contents among several daughter cells. During this process, the plasma membrane is pulled down around each cell. The plasma membrane does not go through these changes during gametocytogenesis, as it undergoes expansion instead of cellular division. Given the striking differences in these transformations, it is unsurprising that while some members of the basal complex are expressed both in the asexual and transmission stages, there are other components that are unique to one or the other. Identification of a protein that is only expressed in gametocytes or only in the asexual-stage basal complex would lead to a better understanding of which components enable these functional differences. In contrast, identification of a protein that is expressed in both asexual and transmission stages would reveal a molecular target for an antimalarial that could both treat a patient and prevent transmission. Through proximity-dependent biotin identification in schizonts and gametocytes, we identified proteins that fulfill both of these conditions. Functional analysis of PfBLEB-proximal proteins will enable the characterization of the compositional and mechanistic differences between schizogony and gametocytogenesis. It is therefore critical to perform detailed studies of the proteins we identified, including PF3D7_1435600, which we have shown to have a unique localization, distinct from PfBLEB in both schizonts and gametocytes.

Early characterizations of *P. falciparum* gametocytes by electron microscopy noted that the nucleus typically resides opposite from the edge where the IMC is initially laid (11). This finding is consistent with our immunofluorescence images, in which the nucleus is consistently located on the same side as PfBLEB. Perhaps PfBLEB or a neighboring protein plays a role in positioning the nucleus within the cell. This hypothesis is worth exploring in future studies.

The IMC and associated microtubules confer rigidity to developing gametocytes (18, 39). It is hypothesized that the rigidity of immature gametocytes aids in their sequestration in the microvasculature of the human host, and thus is important for their ability to avoid splenic clearance (39). It is possible that disruption of PfBLEB, through disruption of the IMC and microtubules, could abolish the rigidity of immature gametocytes, which may inhibit sequestration, thus exposing them to splenic clearance. Inhibition of PfBLEB or its interacting partners could therefore provide an angle to both prevent gametocyte maturation and block sequestration of immature gametocytes. Interestingly, our results also demonstrate an important role for the IMC and associated microtubules for survival of the developing gametocyte independent of sequestration or host immune system evasion.

Despite the importance of gametocytes in malaria transmission, many of the molecular mechanisms involved in parasite cellular and structural remodeling are largely unknown. Drugs that target the development of gametocytes could be used to block transmission. Inhibitors of the basal complex that disrupt IMC formation have potential as multistage antimalarials that target both asexual- and transmission-stage parasites.

The major function of the IMC network in gametocytes is to generate and maintain cell shape (18). *P. falciparum* is unique within the *Plasmodium* genus in that it is the only species to undergo the dramatic transformation into a crescent shape (reviewed by Ngotho et al. (12)). A handful of early electron microscopic studies suggest that the IMC in *P. berghei* and *P. knowlesi* does not completely surround these round gametocytes and instead lays discontinuously around the perimeter of the cell (40, 41). This suggests that *Plasmodium* species with

round gametocytes may not require a stable or continuous IMC, and therefore may not require BLEB in the development of transmission stages. Intriguingly, we have demonstrated that PyBLEB is expressed on the periphery of nonfalciform *P. yoelii* gametocytes (*SI Appendix*, Fig. S4), but its function remains unclear. Future investigations into the IMC, BLEB, and its interacting partners in nonfalciform gametocytes may clarify how the development of transmission stages varies between species.

MORN1 has been shown to localize to the site of budding and the anterior end of the microgamete of *Toxoplasma gondii, Eimeria acervulina, E. tenella, and E. maxima (29)*, but no studies have assessed the localization of other basal complex proteins or probed the function or localization of MORN1 in sexual or presexual stages of *P. falciparum*. While we do not observe PfMORN1 expression via immunofluorescence during the development of *P. falciparum* gametocytes, it is possible that PfMORN1 or another basal complex protein plays a role in fully mature gametes.

As PfBLEB is unique to *Plasmodium* spp., it may serve as a useful tool with which to reveal differences in segmentation and sexual conversion of *Plasmodium* compared to other apicomplexans including *Toxoplasma*. It has previously been shown that PfBTP1 and PfCINCH do not have orthologs outside of *Plasmodium* (20, 22). The information we share in this study further adds to the body of evidence that many components of the basal complex, including PfBLEB, are not broadly conserved among apicomplexan parasites.

Eradication of malaria requires knowledge of the critical biological processes of the *P. falciparum* parasite. We have discovered a novel basal complex protein, PfBLEB, and have demonstrated evidence for a key role in gametocyte maturation. Furthermore, we have identified proteins that are in close proximity to PfBLEB during schizogony and/or gametocytogenesis that are promising targets for future studies. The information gained from this study reveals novel parasite biology and may shed light on potential drug targets.

Materials and Methods

Reagents and Antibodies. Primers were obtained from Integrated DNA Technologies or Life Technologies; restriction enzymes were obtained from New England Biolabs. Commercially available antibodies were obtained from Sigma (rat anti-hemagglutinin [HA] [clone 3F10] and mouse anti-tubulin [clone B-5-1-2]), Bio-Rad (mouse anti-V5, clone SV5-Pk2), Abcam (rabbit anti-histone H3 [ab1971]), and Jackson ImmunoResearch (mouse anti-biotin, clone 3D6.6). Mouse anti-Myc (clone 9E10) was obtained from the Brigham and Women's Hospital-Brigham Research Institute Antibody Core Facility. PfMORN1 and PfBCP1 antisera were obtained as previously described (22), as were *P. yoelii* dynein heavy-chain delta domain (DDD) (42) and PyCITH (43). Rabbit polyclonal antisera against recombinant GST-PyMSP1 (AA1619-1754, expressed in *Escherichia coli* BL21(DE3)pLysS codon plus with plasmid pSL1331) was generated by Pocono Rabbit Farm & Laboratory. Other antibodies were kindly provided by Alan Cowman, Jenny Thompson, and Kaye Wycherley at The Walter & Eliza Hall Institute of Medical Research (Melbourne, Australia) (mouse anti-PfRON4) (44) and Julian Rayner at the University of Cambridge (rabbit anti-PfGAP45) (45).

***Plasmodium falciparum* Culture and Transfection.** See *SI Appendix*, *Supplementary Materials and Methods*.

Experimental Animals. See *SI Appendix*, *Supplementary Materials and Methods*.

Reverse Genetics of *P. yoelii* 17XNL Parasites. See *SI Appendix*, *Supplementary Materials and Methods*.

Plasmid Construction. See *SI Appendix*, *Supplementary Materials and Methods*.

Immunofluorescence Microscopy. Immunofluorescence microscopy was performed on slides with 4% vol/vol paraformaldehyde-fixed *P. falciparum* parasites. Following an initial air-drying step, slides were kept in a humid chamber during the entire process. Parasites were permeabilized with 0.1% vol/vol Triton X-100 for 10 min and blocked with 3% wt/vol bovine serum albumin (BSA) for 1 h at RT. Primary antibodies were incubated for 1 h at RT in the following dilutions: anti-V5 (1:500), anti-PfMORN1 (1:2,000), anti-PfGAP45 (1:5,000), anti-HA (1:50), anti-PfRON4 (1:200), anti-PfBCP1 (1:2,500), anti-Myc (1:100), anti-α-tubulin (1:1,000), and/or anti-biotin (1:200). Subsequently, cells were washed three times with PBS and incubated for 30 min with AlexaFluor 488, 555, 594, or 647 secondary antibodies (1:1,000; Life Technologies). After removal of the unbound antibodies with three PBS washes, slides were mounted with Vectashield containing DAPI (Vector Laboratories) with coverslips and kept at 4 °C until evaluation. Superresolution-structured illumination microscopy (SR-SIM) z stacks were captured using an ELYRA PS.1 microscope (Carl Zeiss Microscopy). The ELYRA was used with a 60× (oil) objective and excitation wavelengths of 405, 488, 561, and 638 nm. SIM images were collected at 50 to 200 nm z axis steps, with 5 rotations of the structured illumination grid per channel. Resulting stacks were processed using default reconstruction parameters in ZEN Black software. Airyscan images were obtained with a Zeiss LSM880 with Airyscan with 60× oil objective (Carl Zeiss Microscopy). Widefield images were obtained on an Olympus BX40 microscope with a 60× or 100× oil objective.

Immunofluorescence microscopy of PyBLEB::GFP parasites was performed on fixed cells as described previously (46). For *P. yoelii* asexual blood stage parasites, the blood of infected mice was collected and cultured ex vivo as described above. For *P. yoelii* sexual stages, mice were infected, and at 1% parasitemia, were provided with 10 mg/L sulfadiazine-medicated drinking water (VWR, catalog no. AAA12370-30) for 48 h. The blood of infected mice was then collected and pelleted at 1,400 × *g* for 3 min. All subsequent centrifugations were performed at this speed and all subsequent steps were performed for both asexual and sexual stages. Cells were fixed in 4% vol/vol paraformaldehyde and 0.0075% vol/vol glutaraldehyde in 1× PBS for 30 min at RT. Cells were washed once in 1× PBS and then permeabilized in 0.1% vol/vol Triton X-100 for 10 min at RT. Cells were washed once in 1× PBS and then blocked in 3% wt/vol BSA overnight at 4 °C. Following blocking, cells were stained with primary antibody (GFP, MSP1, CITH, DDD, diluted 1:1,000) for 1 h at RT or overnight at 4 °C. Cells were then washed twice with 3% wt/vol BSA in 1× PBS and then stained with species-specific secondary antibodies conjugated to Alexa Fluor 488 and 594 (both 1:2,000) for 1 h at RT. Cells were washed in 1× PBS and then stained with DAPI (1 μg/mL) for 5 min at RT. Cells were washed twice in 1× PBS before resuspending in 1× PBS before mounting (50 μL 1× PBS for sexual stages and 200 μL 1× PBS for asexual stages) onto glass slides in Prolong-Gold Anti Fade mounting medium at a 1:1 ratio and immediately covered with a glass coverslip. After settling for 10 min, slides were sealed with nail polish and stored at RT until imaging. The VT-iSIM microscope (BioVision) with a 100× (oil) objective was used for high-resolution image capture of z slices every 1 μm with MetaMorph software, and the z slices were deconvolved using the Microvolution plug-in on ImageJ (NIH).

Live-Cell Microscopy. PfBLEB-HaloTag/PfCINCH-mNeonGreen parasites were purified at the schizont stage by density centrifugation with 60% Percoll. Purified schizonts were incubated with 200 nM JaneliaFluor 646 HaloTag ligand (Promega) for 30 min, washed with media, and plated on a 60-mm glass-bottom dish, which had been pretreated with concanavalin A for 1 h at 37 °C. Parasites were allowed to settle for 30 min, and then unbound cells were washed off with PBS. The dish was filled with complete phenol red-free RPMI 1640 and imaged using the Zeiss Elyra7 with Lattice SIM^2 with 63× oil objective with heated stage.

Gametocyte Induction and Staging of PfBLEB-smV5^{Tet} and PfBLEB^{KO} Parasites. Trophozoite-stage parasites ± ATc at 0.25% parasitemia were plated with 50% conditioned AlbuMAX II medium to a final 2% hematocrit. After 2 d, the newly invaded ring parasitemia was determined using flow cytometry and 0.25 mg/mL heparin (Alpha Aesar A16198) was added to prevent subsequent reinvasion of asexual stage parasites, allowing monitoring of gametocyte formation. Gametocytemia (day 6) and gametocyte morphology (days 8 to 12) were assayed by light microscopy of thin blood smear stained with Hemacolor (Sigma) staining solution. A total of 800 RBCs (gametocytemia) or 50 gametocytes (morphology and staging) were counted per replicate. The gametocyte conversion rate was calculated as gametocytemia on day 6 divided by ring parasitemia on day 2. IFAs were performed on days 4 to 12 as indicated.

Gametocyte Viability. PfBLEB knockout parasites or wild-type 3D7 parasites were induced as described above. Beginning 6 d postinduction, gametocyte viability was assessed using the BacTiter-Glo Microbial Cell Viability assay (Promega), which quantifies adenosine triphosphate (ATP) levels using a luminescent output. Luminescence levels of an uninfected RBC control were subtracted, and then values were normalized to the average luminescence of 3D7 parasites on each day and gametocytemia for each well. Unpaired *t* tests were performed on each day indicated using GraphPad Prism.

Exflagellation Assay. PfBLEB knockout parasites or wild-type 3D7 parasites were induced as described above. At 14 d postinduction, exflagellation capacity was assessed by incubating gametocytes for 15 min at RT in 100 μM xanthurenic acid (Sigma). Following incubation, cells were fixed for immunofluorescence microscopy as described above with anti-α-tubulin antibody. Cells were visualized with an Olympus BX40 widefield microscope and a 60× oil objective. For each replicate, 50 fields were randomly selected and the total number of α-tubulin$^+$ exflagellation centers was counted. Unpaired *t* test was performed using GraphPad Prism.

Flow Cytometry Analysis of Parasite Replication. Parasites were synchronized at the ring stage with 5% wt/vol sorbitol. Parasites grown in ATc were washed 3× for 10 min at 37 °C in fresh media. Cultures were plated in triplicate at 0.25% parasitemia and incubated at 37 °C at a hematocrit of 2% in the presence or absence of ATc. For each time point, 100 μL culture was plated in triplicate into a U-Bottom 96-well plate. Cells were washed with a 0.5% wt/vol BSA-PBS solution. Cells were then incubated with 100 μL 1:1,000 SYBR Green I (Life Technologies) for 20 min at RT. Cells were washed with 0.5% BSA-PBS solution and resuspended in PBS. Flow cytometry data were collected using a BD FACSCalibur (BD Biosciences) with an acquisition of 100,000 events per sample. Initial gating was carried out with unstained, uninfected erythrocytes to account for erythrocyte autofluorescence.

Western Blot. *P. falciparum* proteins were extracted using 0.2% wt/vol saponin and pellets were resuspended in Laemmli sample buffer and boiled for 10 min at 70 °C. All of the protein samples were separated on 10% mini-Protean TGX gels (Bio-Rad) and transferred to nitrocellulose membranes using wet transfer with low methanol at 45 V for 2.5 h. Membranes were probed with primary antibodies in the following dilutions: anti-V5 (1:3,000) and anti-histone H3 (1:2,500) in TBST. Primary antibody binding was detected using secondary antibodies directly labeled with near-infrared dyes (at a 1:10,000 dilution, LiCor). Quantification of immunoblot data was performed using volumetric measurement of fluorescence intensity on a LiCor Odyssey CLx imager.

TEM. PfBLEB-smV5^{Tet} gametocytes were induced with or without ATc as described above and purified using MACS magnetic columns 5 or 8 d postinduction. Parasites were resuspended in fixative (2.5% vol/vol paraformaldehyde, 5% vol/vol glutaraldehyde, and 0.06% vol/vol picric acid in 0.2 M cacodylate buffer) and subjected to standard TEM preparation and visualized on a JEOL1200EX.

Proximity-Dependent Biotinylation of Schizonts. 3D7-PfBLEB-TurboID parasites were tightly synchronized by density centrifugation with 60% vol/vol Percoll, allowed to reinvade fresh erythrocytes for 2 to 3 h, and new rings were isolated with 5% (wt/vol) sorbitol. Synchronized parasites were expanded to 500 mL at ∼3% schizontemia. At ∼46 h postinvasion, parasites were treated with 2.5 μM compound 1 (4-[2-(4-fluorophenyl)-5-(1-methylpiperidine-4-yl)-1H-pyrrol-3-yl]pyridine) for 1 h. DMSO or 150 μM biotin was added to the synchronized schizonts for 1 h. At collection, RBCs were lysed with 0.05% wt/vol saponin in PBS with protease inhibitors (SigmaFast Protease Inhibitor Mixture, Sigma). Parasite pellets were lysed in RIPA (50 mM Tris·HCl, pH 7.5, 150 mM NaCl, 1% Nonidet P-40, 0.5% sodium deoxycholate, 0.1% sodium dodecyl sulfate) plus protease inhibitor for 30 min on ice, sonicated twice at 20% amplitude for 30 s, and insoluble material was removed by centrifugation. Parasite lysate was applied to magnetic streptavidin-coated beads (ThermoFisher) and incubated for 2.5 h at 4 °C. Beads were washed with fresh RIPA plus protease inhibitors, 2% wt/vol SDS, 50 mM HEPES pH 7.5/500 mM NaCl/L mM EDTA/1% vol/vol Triton-X 100/0.1% wt/vol sodium deoxycholate, 10 mM Tris·HCl pH 8.0/250 mM lithium chloride/1 mM EDTA/0.5% vol/vol Nonidet P-40/0.5% wt/vol sodium deoxycholate, resuspended in 40 μL 50 mM ammonium bicarbonate, and submitted for detergent removal, on-bead digestion, and mass spectrometry analysis. Mass spectrometry results were analyzed by comparing the number of unique and total peptides present in experimental and control samples.

Proximity-Dependent Biotinylation of Gametocytes. NF54-PfBLEB-TurboID gametocytes were induced at scale as previously described (47). Parasites were cultured in biotin-free (first replicate) or biotin-containing (second replicate) media for multiple cycles. Approximately 500 mL 1 to 2% ring-stage parasites were switched to biotin-free media ∼20 h before gametocyte induction. At ∼26 to 28 h postinvasion, parasites were washed once in biotin-free RPMI media and once in minimal fatty acid (mFA) media (RPMI, sodium bicarbonate, fatty acid-free bovine serum albumin, 30 μM oleic acid, 30 μM palmitic acid). They were then incubated in mFA media for roughly 24 h and switched back to complete biotin-free RPMI. On day 2 postinduction, 0.25 mg/mL heparin and 50 mM GlcNAc were added to the media. On days 3 to 5 postinduction, 0.25 mg/mL heparin was added to the media. On day 5 postinduction, stages II and III gametocytes were treated with DMSO or 150 μM biotin for 2 to 3 h and collected for analysis as described above.

Localization of PF3D7_1435600-smV5 in Gametocytes. To visualize the localization of PF3D7_1435600 in gametocytes, sexual stages were induced with a modified crash method (48). Briefly, parasites were synchronized to 5 to 6% rings. At ∼32 to 40 hpi, 2/3 of the media was replaced with fresh media. After an additional 24 h, media was completely changed with fresh media every day for 10 d. Two days after induction, heparin was added at 0.25 mg/mL for 2 to 3 d to prevent reinvasion of asexual stages.

Data Availability. fastq files data have been deposited in the NCBI Sequence Read Archive (PRJNA813841) (49). All of the study data are included in the article and/or supporting information.

ACKNOWLEDGMENTS. We thank Matthias Marti, Deepali Ravel, and Ana Rita Batista Gomes for sharing their knowledge of gametocyte culturing; Maria Ericsson at the Harvard Electron Microscopy Facility for help with TEM; and Dr. and Mrs. Daniel Simmons for their support of microscopy at the Harvard Center for Biological Imaging. This work was supported by National Institutes of Health R01-AI145941 (to J.D.D.), R01-AI169648 (to J.D.D.), and T32-HD055148 (to V.A.S.).

Author affiliations: [a]Biological and Biomedical Sciences, Harvard Medical School, Boston, MA 02115; [b]Division of Infectious Diseases, Boston Children's Hospital, Boston, MA 02115; [c]Department of Biochemistry and Molecular Biology, the Huck Center for Malaria Research, Pennsylvania State University, University Park, PA 16802; and [d]Department of Pediatrics, Harvard Medical School, Boston, MA 02115

1. World Health Organization, World malaria report 2021. https://www.who.int/teams/global-malaria-programme/reports/world-malaria-report-2021. Accessed 1 July 2022.
2. A. F. Cowman, J. Healer, D. Marapana, K. Marsh, Malaria: Biology and disease. *Cell* **167**, 610–624 (2016).
3. E. H. Ekland, D. A. Fidock, In vitro evaluations of antimalarial drugs and their relevance to clinical outcomes. *Int. J. Parasitol.* **38**, 743–747 (2008).
4. WHO, *Global Report on Antimalarial Drug Efficacy and Drug Resistance: 2000–2010* (World Health Organization, Geneva, Switzerland, 2010).
5. J. B. Koenderink, R. A. Kavishe, S. R. Rijpma, F. G. Russel, The ABCs of multidrug resistance in malaria. *Trends Parasitol.* **26**, 440–446 (2010).
6. T. N. Wells, R. Hooft van Huijsduijnen, W. C. Van Voorhis, Malaria medicines: A glass half full? *Nat. Rev. Drug Discov.* **14**, 424–442 (2015).
7. E. Meibalan, M. Marti, Biology of malaria transmission. *Cold Spring Harb. Perspect. Med.* **7**, a025452 (2017).
8. R. M. Rudlaff, S. Kraemer, J. Marshman, J. D. Dvorin, Three-dimensional ultrastructure of *Plasmodium falciparum* throughout cytokinesis. *PLoS Pathog.* **16**, e1008587 (2020).
9. M. E. Francia, B. Striepen, Cell division in apicomplexan parasites. *Nat. Rev. Microbiol.* **12**, 125–136 (2014).
10. F. Hawking, M. E. Wilson, K. Gammage, Evidence for cyclic development and short-lived maturity in the gametocytes of *Plasmodium falciparum*. *Trans. R. Soc. Trop. Med. Hyg.* **65**, 549–559 (1971).
11. R. E. Sinden, Gametocytogenesis of *Plasmodium falciparum* in vitro: An electron microscopic study. *Parasitology* **84**, 1–11 (1982).
12. P. Ngotho *et al.*, Revisiting gametocyte biology in malaria parasites. *FEMS Microbiol. Rev.* **43**, 401–414 (2019).
13. M. Kono, D. Prusty, J. Parkinson, T. W. Gilberger, The apicomplexan inner membrane complex. *Front. Biosci.* **18**, 982–992 (2013).
14. H. E. Bullen *et al.*, A novel family of Apicomplexan glideosome-associated proteins with an inner membrane-anchoring role. *J. Biol. Chem.* **284**, 25353–25363 (2009).

15. M. K. Dearnley *et al.*, Origin, composition, organization and function of the inner membrane complex of *Plasmodium falciparum* gametocytes. *J. Cell Sci.* **125**, 2053–2063 (2012).
16. M. Kono *et al.*, Evolution and architecture of the inner membrane complex in asexual and sexual stages of the malaria parasite. *Mol. Biol. Evol.* **29**, 2113–2132 (2012).
17. S. Absalon, J. A. Robbins, J. D. Dvorin, An essential malaria protein defines the architecture of blood-stage and transmission-stage parasites. *Nat. Commun.* **7**, 11449 (2016).
18. M. Parkyn Schneider *et al.*, Disrupting assembly of the inner membrane complex blocks *Plasmodium falciparum* sexual stage development. *PLoS Pathog.* **13**, e1006659 (2017).
19. M. W. Dixon, M. K. Dearnley, E. Hanssen, T. Gilberger, L. Tilley, Shape-shifting gametocytes: How and why does *P. falciparum* go banana-shaped? *Trends Parasitol.* **28**, 471–478 (2012).
20. M. Kono *et al.*, Pellicle formation in the malaria parasite. *J. Cell Sci.* **129**, 673–680 (2016).
21. C. J. Moran, J. D. Dvorin, The basal complex protein PfMORN1 is not required for asexual replication of *Plasmodium falciparum*. *MSphere* **6**, e0089521 (2021).
22. R. M. Rudlaff, S. Kraemer, V. A. Streva, J. D. Dvorin, An essential contractile ring protein controls cell division in *Plasmodium falciparum*. *Nat. Commun.* **10**, 2181 (2019).
23. K. Engelberg *et al.*, A MORN1-associated HAD phosphatase in the basal complex is essential for *Toxoplasma gondii* daughter budding. *Cell. Microbiol.* **18**, 1153–1171 (2016).
24. B. R. Anderson-White *et al.*, A family of intermediate filament-like proteins is sequentially assembled into the cytoskeleton of *Toxoplasma gondii*. *Cell. Microbiol.* **13**, 18–31 (2011).
25. M. J. Gubbels, S. Vaishnava, N. Boot, J. F. Dubremetz, B. Striepen, A MORN-repeat protein is a dynamic component of the *Toxoplasma gondii* cell division apparatus. *J. Cell Sci.* **119**, 2236–2245 (2006).
26. K. Hu *et al.*, Cytoskeletal components of an invasion machine–The apical complex of Toxoplasma gondii. *PLoS Pathog.* **2**, e13 (2006).
27. A. Lorestani *et al.*, A Toxoplasma MORN1 null mutant undergoes repeated divisions but is defective in basal assembly, apicoplast division and cytokinesis. *PLoS One* **5**, e12302 (2010).
28. A. T. Heaslip, F. Dzierszinski, B. Stein, K. Hu, TgMORN1 is a key organizer for the basal complex of Toxoplasma gondii. *PLoS Pathog.* **6**, e1000754 (2010).
29. D. J. Ferguson *et al.*, MORN1 has a conserved role in asexual and sexual development across the apicomplexa. *Eukaryot. Cell* **7**, 698–711 (2008).
30. C. Aurrecoechea *et al.*, PlasmoDB: A functional genomic database for malaria parasites. *Nucleic Acids Res.* **37**, D539–D543 (2009).
31. F. Chen, A. J. Mackey, C. J. Stoeckert, Jr, D. S. Roos, M. C. L.-D. B. Ortho, OrthoMCL-DB: Querying a comprehensive multi-species collection of ortholog groups. *Nucleic Acids Res.* **34**, D363–D368 (2006).
32. S. Viswanathan *et al.*, High-performance probes for light and electron microscopy. *Nat. Methods* **12**, 568–576 (2015).
33. S. M. Ganesan, A. Falla, S. J. Goldfless, A. S. Nasamu, J. C. Niles, Synthetic RNA-protein modules integrated with native translation mechanisms to control gene expression in malaria parasites. *Nat. Commun.* **7**, 10727 (2016).
34. J. Birnbaum *et al.*, A genetic system to study *Plasmodium falciparum* protein function. *Nat. Methods* **14**, 450–456 (2017).
35. M. Zhang *et al.*, Uncovering the essential genes of the human malaria parasite *Plasmodium falciparum* by saturation mutagenesis. *Science* **360**, eaap7847 (2018).
36. E. Lasonder *et al.*, Integrated transcriptomic and proteomic analyses of *P. falciparum* gametocytes: Molecular insight into sex-specific processes and translational repression. *Nucleic Acids Res.* **44**, 6087–6101 (2016).
37. T. C. Branon *et al.*, Efficient proximity labeling in living cells and organisms with TurboID. *Nat. Biotechnol.* **36**, 880–887 (2018).
38. T. Hulsen, BioVenn–An R and Python package for the comparison and visualization of biological lists using area-proportional Venn diagrams. *Lect. Notes Comput. Sci.* **4**, 51–61 (2021).
39. M. Aingaran *et al.*, Host cell deformability is linked to transmission in the human malaria parasite *Plasmodium falciparum*. *Cell. Microbiol.* **14**, 983–993 (2012).
40. M. Aikawa, C. G. Huff, H. Sprinz, Comparative fine structure study of the gametocytes of avian, reptilian, and mammalian malarial parasites. *J. Ultrastruct. Res.* **26**, 316–331 (1969).
41. B. Mons, Intra erythrocytic differentiation of *Plasmodium berghei*. *Acta Leiden.* **54**, 1–124 (1986).
42. K. J. Hart *et al.*, Plasmodium male gametocyte development and transmission are critically regulated by the two putative deadenylases of the CAF1/CCR4/NOT complex. *PLoS Pathog.* **15**, e1007164 (2019).
43. S. Bennink *et al.*, A seven-helix protein constitutes stress granules crucial for regulating translation during human-to-mosquito transmission of *Plasmodium falciparum*. *PLoS Pathog.* **14**, e1007249 (2018).
44. D. Richard *et al.*, Interaction between *Plasmodium falciparum* apical membrane antigen 1 and the rhoptry neck protein complex defines a key step in the erythrocyte invasion process of malaria parasites. *J. Biol. Chem.* **285**, 14815–14822 (2010).
45. M. L. Jones, C. Cottingham, J. C. Rayner, Effects of calcium signaling on *Plasmodium falciparum* erythrocyte invasion and post-translational modification of gliding-associated protein 45 (PfGAP45). *Mol. Biochem. Parasitol.* **168**, 55–62 (2009).
46. L. M. Bowman, L. E. Finger, K. J. Hart, S. E. Lindner, Definition of constitutive and stage-enriched promoters in the rodent malaria parasite, *Plasmodium yoelii*. *Malar. J.* **19**, 424 (2020).
47. N. M. B. Brancucci *et al.*, Lysophosphatidylcholine regulates sexual stage differentiation in the human malaria parasite *Plasmodium falciparum*. *Cell* **171**, 1532–1544.e1515 (2017).
48. Q. L. Fivelman *et al.*, Improved synchronous production of *Plasmodium falciparum* gametocytes in vitro. *Mol. Biochem. Parasitol.* **154**, 119–123 (2007).
49. R. L. Clements *et al.*, Raw illumina sequencing reads for 3D7-JDD342.1. NCBI Sequence Read Archive. https://www.ncbi.nlm.nih.gov/sra/?term=PRJNA813841. Accessed 4 August 2022.